Journal of Nonlinear Optical Physics & Materials
Vol. 11, No. 4 (2002) 433–443

NONLINEAR QUANTUM WELL INFRARED PHOTODETECTOR

H. C. LIU* and E. DUPONT
Institute for Microstructural Sciences,
National Research Council, Ottawa, Ontario K1A 0R6, Canada
**h.c.liu@nrc.ca*

M. ERSHOV
PDF Solutions, 333 West San Carlos Street, San Jose, CA 95110, USA

Received 24 October 2002

Nonlinear processes in quantum well infrared photodetectors (QWIP) are reviewed. Being an intersubband dipole transition based photoconductor, the nonlinear behaviors in QWIPs are caused by both the (extrinsic) photoconductive transport mechanism and (intrinsic) nonlinear optical processes. Extrinsic nonlinearity leads to a degradation of QWIP performance at high incident power or low operating temperatures. Some intrinsic nonlinear QWIP properties are useful in applications, such as in autocorrelation of short pulses by two-photon absorption. The general area of QWIP nonlinear properties has not been extensively investigated. We point out some directions for further studies and hope to stimulate more research activities.

Keywords: Quantum well; infrared; photodetector; intersubband; high speed; high frequency.

1. Introduction

The quantum well infrared photodetector (QWIP) is best known for its application in infrared detection and thermal imaging.[1,2] A large number of publications have been devoted to the studies of device physics and optimization. For these standard applications, the device parameters are chosen to have the highest sensitivity and operating temperature for the detection of weak signals. In a different direction involving commonly a laser, a strong infrared excitation is present. Only limited works have been carried in this area.[3–5] The study of QWIPs under strong illuminations is relevant to a number of applications such as heterodyne detection,[6] infrared pulse characterization,[7,8] and free space optical communication.[9,10] In view of the high intrinsic speed[11] and the recent demonstration of near ideal absorption efficiency,[12,13] QWIPs are well suited for these more exploratory applications.

This paper reviews the physics and understanding of QWIPs under strong illumination and points out areas of further study and opportunity. We stress at the onset that this area has not been extensively studied, and hence a comprehensive

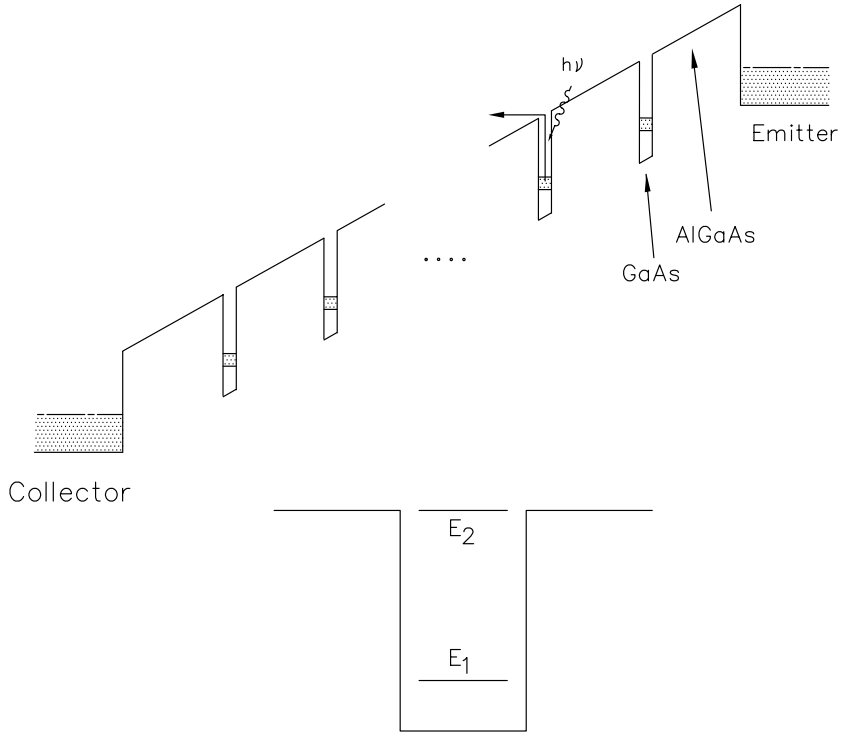

Fig. 1. Schematic conduction bandedge profile of a GaAs/AlGaAs QWIP under an applied bias voltage (above) and of the flatband single well, i.e. the period of the multi-QW structure (below). The electron population in the n-type wells is provided by doping using silicon. The emitter and collector contact layers are of the same n-type, doped with silicon. Photons ($h\nu$) excite electrons from quantum wells, causing a photocurrent. The ground and first excited states are labeled by E_1 and E_2, respectively. To facilitate a rapid escape of photoexcited electrons, E_2 is designed to be either very close to the top of the barrier or in the continuum. Usually many wells (10–100) are required for sufficient absorption.

review is not possible. We hope, however, that this paper will stimulate further studies.

Before going into the details of discussing the nonlinear properties and for completeness, the basic QWIP operation principles are summarized briefly. We present the simplest picture of a QWIP made of n-type GaAs/AlGaAs in Fig. 1. The detector operation is based on photo-emission of electrons from the quantum wells. The device is essentially a unipolar photoconductor. A detailed discussion of the QWIP physics is found in Ref. 1.

2. Extrinsic (Photoconductive) Nonlinearity

An ideal photoconductor has a responsivity independent of the illumination power if the power is low, i.e. photocurrent is linearly proportional to power. The dependence of responsivity on the fundamental QWIP parameters is given by the standard

expression[1]:

$$R(E) = \frac{e}{h\nu}\eta_0 g(E) = \frac{e}{h\nu}\eta_0 p_e(E)\frac{\tau_c(E)}{\tau_{tr}(E)} \quad (1)$$

where $h\nu$ is the photon energy, η_0 is the total absorption quantum efficiency, g is the photocurrent gain, p_e is the photoexcited carrier escape probability, τ_c is the photoexcited carrier lifetime, and τ_{tr} is the transit time across QWIP ($\tau_{tr} = L/v(E)$, where L is the QWIP length, and v is the drift velocity). In an idealized case, the electric field E across QWIP is constant and equals to $E_0 = V/L$, where V is the applied voltage. This condition is satisfied in QWIPs with a large number of equally doped QWs at low excitation power. The condition that the electric field is constant and independent of the illumination power can be violated at high incident power due to several reasons.

2.1. *Contact effects*

Under uniform QW excitation (including both thermo- and photo-excitation) the electric field in QWIPs with multiple QWs is constant in the bulk of the detector.[14,15] However, the balance between the injection from the emitter and the bulk current in the steady-state leads to the creation of a high electric field domain near the injection contact.[14] QWs in the bulk of QWIP are electrically neutral (QW electron density equals to QW doping), while a few (2–5) QWs near the emitter are partially depleted to provide high contact electric field required for injection. At high illumination power, the total current and injection current may become so high that the voltage drop across the high field domain becomes comparable with the total applied voltage. This leads to a reduction of the electric field in the bulk of QWIP (since the total voltage is kept constant), and hence to a decrease of the escape probability and an increase of the transit time (due to the decreased drift velocity). As a result, the responsivity is decreased at high power and the photocurrent may saturate with power. These effects, investigated in detail in Ref. 5, are illustrated in Fig. 2. Experiments were conducted on standard 9-μm QWIPs at 77 K (non-background limited) using a CO_2 laser. The experimental results were explained by self-consistent numerical simulations. For these experiments, the nonlinearity was observed at a power level greater than about 1 W/cm^2, and the power was increased up to about 1000 W/cm^2. With a CW CO_2 laser we did not observe any damage to the device. This property of laser "hardness" is quite unique to QWIPs, especially in view of the low damage threshold (1 W/cm^2) of the standard infrared detectors made of HgCdTe. This hardness in resisting high power illumination is an advantageous property for heterodyne detection. With the recent demonstration of near 100% absorption efficiencies,[12,13] QWIPs are ideally suited for heterodyne detection.[6] Thus, the first mechanism of high power QWIP nonlinearity is related to the contact effects and modulation (reduction) of the bulk electric field in QWIPs. This mechanism is revealed much more strongly in QWIPs with a small number of QWs, where the role of the contact effects is especially

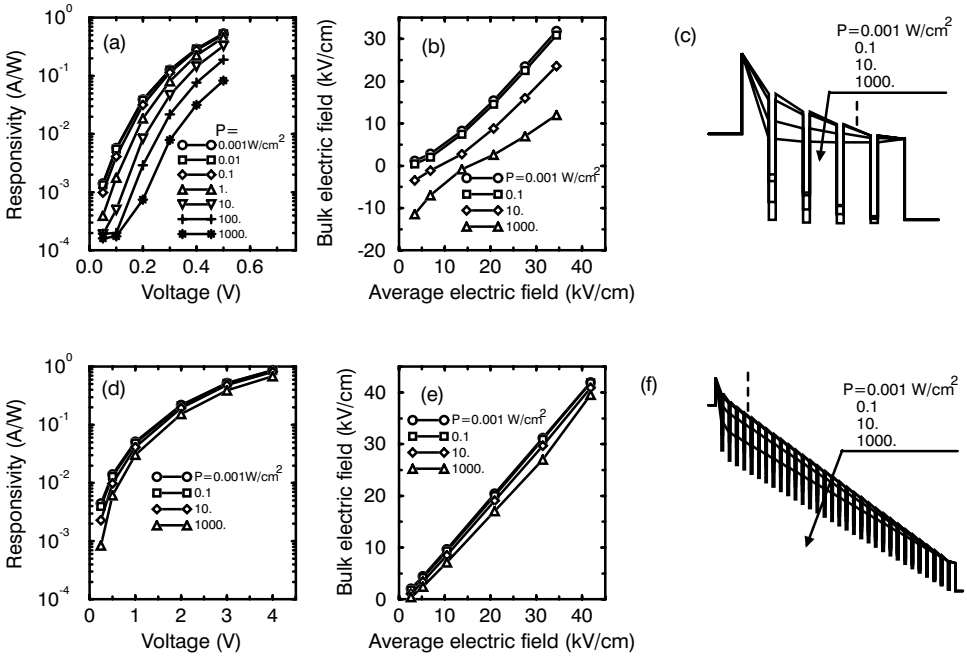

Fig. 2. Simulation results for (a)–(c) 4-well and (d)–(f) 32-well QWIPs under different infrared illumination power densities: (a) and (d) responsivity versus voltage, (b) and (e) electric field in the bulk versus average field, and (c) and (f) conduction bandedge profile at an average field of 15 kV/cm. Values of the bulk field were taken at positions shown by the dashed lines in (c) and (f).

important.[14] Contact related nonlinearity appears to be relatively unimportant in QWIPs with many QWs (> 10),[16] where the voltage drop on the high field domain is small compared with the total applied voltage. It should be noted that in this mode of nonlinearity Eq. (1) and other classic formulas for ideal photoconductor are still applicable, but the electric field E entering these formulas becomes lower than the average electric field $E_0 = V/L$.

2.2. *Non-uniform optical field distribution*

Another mechanism of nonlinearity is due to a non-uniform optical field distribution in QWIPs.[17] The non-uniformity may be caused by the attenuation of the optical power due to absorption.[18] This effect may be pronounced in QWIPs optimized for heterodyne operation, because they have much higher QW doping[12,13] and hence higher absorption than QWIPs designed for low-temperature and low-power applications. Optical power non-uniformity may also be caused by IR radiation reflection form the top metal contact or sidewalls and by interference. The monochromatic light could lead to strong interference patterns in a given experimental geometry. For example, with a polished 45-degree facet coupled QWIP,[19] the standing wave

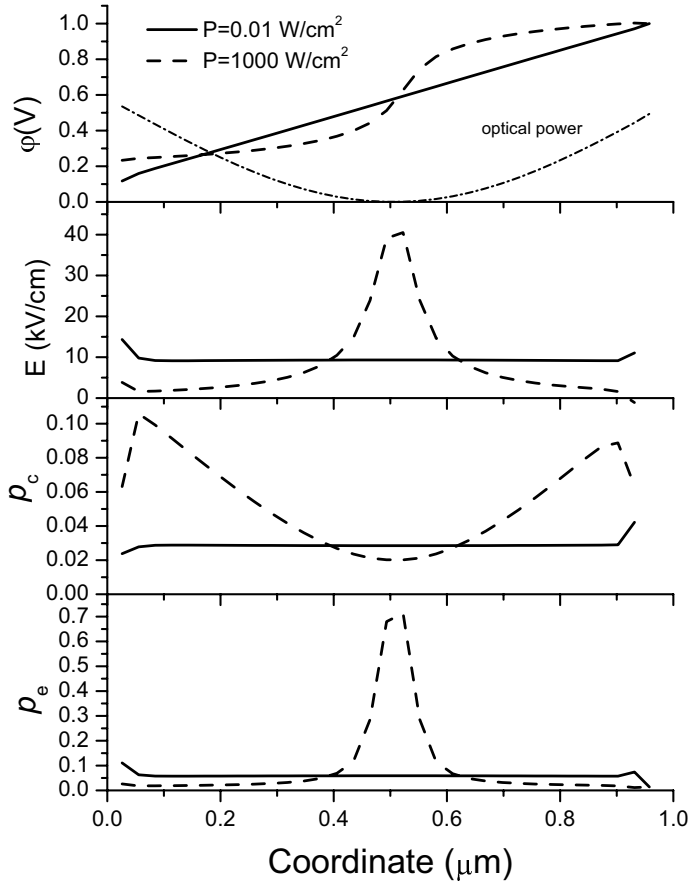

Fig. 3. Coordinate dependence of (a) potential, (b) electric field, (c) QW capture probability, and (d) photoexcited electron escape probability for low-power (solid line) and high-power (dashed line) densities, all for a 32-well QWIP at temperature $T = 77$ K and applied voltage $V = 1$ V. The dash-dotted line shows the distribution of optical power.

pattern leads to a strongly non-uniform illumination. This non-uniform distribution of the optical power leads to a coordinate-dependent photoexcitation rate from the QWs and, therefore, to a non-uniform concentration of the photoexcited carriers. If the non-uniform photoexcitation rate exceeds thermal or background excitation, the current continuity can no longer be provided by a constant electric field across QWIP. The electric field readjusts itself so that the field is increased in regions with low optical power, and decreased where the optical intensity is high (this effect is illustrated in Fig. 3 from Ref. 17). The electric field distribution becomes non-uniform, making invalid the simple standard formulas for responsivity, noise, etc. The non-uniformity of the electric field is supported by a slight recharging of the QWs. Theoretical calculation of detector characteristics in this case requires self-consistent modeling. Photoconductive noise and detector responsivity decrease,

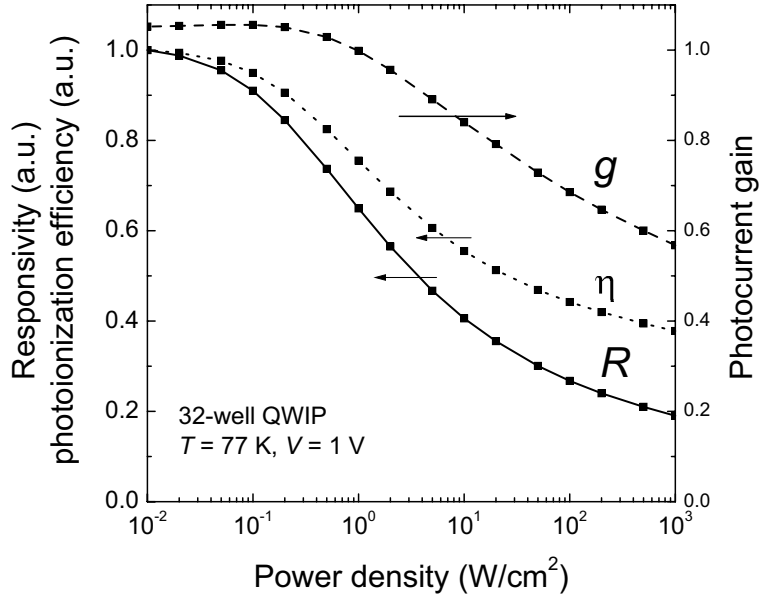

Fig. 4. Responsivity R, photocurrent gain g, and photoemission efficiency $\eta = \eta_0 p_e$ versus incident infrared power.

while the noise gain and noise power are increased with respect to the uniform electric field case (see Fig. 4 from Ref. 17). QWIP nonlinearity due to non-uniform optical power distribution takes place when the photocurrent exceeds the dark current or the background current.

2.3. *Quantum well depletion*

In the steady-state regime considered above, the variation of the QW electron density with incident power is not significant (unless the number of QWs is very small), so that the depletion of the QWs by electrons causes a negligible reduction in the absorption efficiency. The situation may be different in the non-equilibrium regime. If a high-power short (picosecond time scale) infrared pulse is incident on QWIP, a significant fraction of electrons is excited from the QWs.[20] On the short time scale, the absorption and the photocurrent may saturate because the electron density in the QWs responsible for the absorption is decreased. Experimental study of these effects allowed to estimate the photoexcited electron lifetime[3,4] and to study the carrier dynamics.[20] The saturation of the absorption and photoconductivity happens at a very high power — over 10–100 MW/cm^2. However, this type of nonlinearity can exist only on a very short time scale (lifetime or transit time), because the photoexcited carriers quickly relax back to the QWs, or exit to the collector (in which case they are quickly replenished by an extra electron injection from the emitter).

Finally, if a QWIP is operated at low temperatures and low backgrounds, so that the total current is low, the nonlinearity can be observed under a low infrared illumination.[21,22] The key factor is the relative magnitudes of the total current and photocurrent. If the photocurrent is a large or dominant fraction of the total current, the response becomes nonlinear.

To conclude this section, extrinsic or photoconductive nonlinearity of QWIPs can be caused by a number of physical phenomena discussed above. These effects are parasitic, i.e. they lead to a deterioration of the detector characteristics (responsivity, noise power, etc.). In addition, detector nonlinearity complicates the calibration procedure. A care must be taken to avoid these effects, whenever possible. The standard formulas describing QWIP characteristics may lead to erroneous results, and the basic detector parameters (photocurrent gain, noise gain, etc.) loose their straightforward physical meanings due to non-uniformity of the electric field.

3. Intrinsic Nonlinearity

With increasing power, the standard nonlinear optical processes become important. For the dipole intersubband transition itself, the full range of nonlinear optical processes should be observable. So far, absorption saturation,[3,4] hole burning,[23] harmonic (including sum[24]) and difference frequency generation,[25] and two-photon and multiphoton absorption[25,26] have been reported. A review of intersubband nonlinear optics in quantum well structures is given in Ref. 25. Here, specific to QWIPs, we describe the two-photon absorption process occurring in QWIPs and its potential applications.

Using the simplest picture of one-dimensionally confined quantum wells, the calculation of two-photon absorption is straightforward. For a simple square quantum well, three configurations are schematically shown in Fig. 5. For a given photon energy, the three configurations correspond to photo-ionization from the ground state to the continuum via an intermediate (1) resonant real state, (2) off-resonant state, and (3) virtual state. The first case is expected to have the highest two-photon absorption efficiency close to that for a true double-resonance case. A high efficiency is the advantage of the resonant case, but the intrinsic time scale would be limited by the intersubband relaxation of the order of 1 ps. With a sufficient detuning (off-resonant) or for the virtual state case, the intrinsic speed of the device could be much faster than 1 ps. A simple calculation[26] in Fig. 6 shows the efficiency versus photon energy for the three cases. As an estimate of the maximum possible efficiency, we can easily evaluate a double-resonance case analytically. For an equally spaced three-level (fictitious) structure and if the photon energy is exactly on resonance ($\hbar\omega = E_2 - E_1 = E_3 - E_2$), the efficiency (for one QW) is

$$\eta^{(2)} = \left(\frac{e^2 h}{4\epsilon_0 n_r C m}\right)^2 \frac{\sin^4\theta}{\cos\theta} n_{2D} f_{23} f_{12} \frac{P}{2\pi^2 \omega \gamma^3}\,, \tag{2}$$

where n_r is the refractive index, m is the effective mass, θ is the angle of incidence, n_{2D} is the two-dimensional electron density, f_{mn} is the oscillator strength between

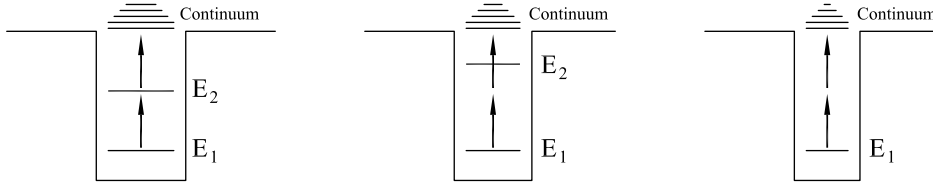

Fig. 5. Schematic two-photon absorption from ground (bound) state to the continuum via an intermediate (left) real resonant state, (center) off-resonant state, and (right) virtual state.

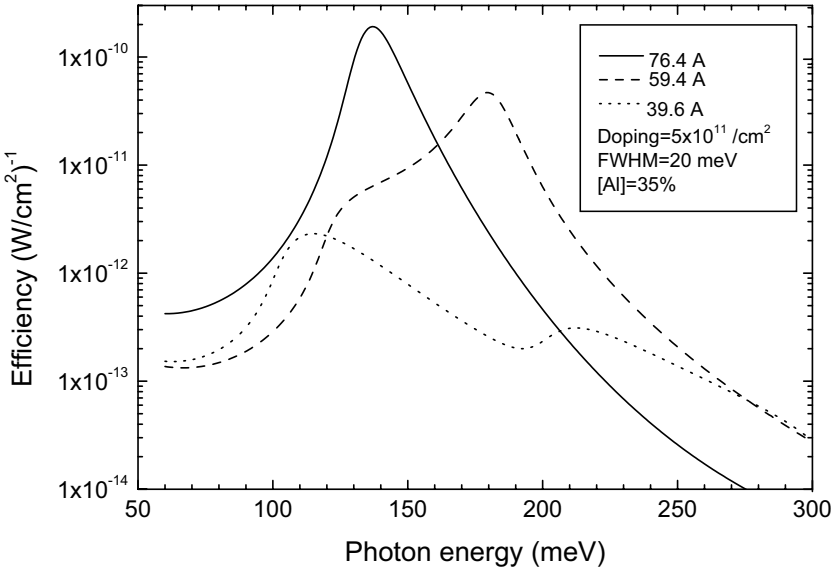

Fig. 6. Calculated two-photon absorption efficiency for three quantum well structures. The GaAs/AlGaAs quantum well parameters are given in the inset. The linewidth parameter is set to be 20 meV. The schematic shown in Fig. 5 corresponds to a photon energy of 136 meV.

m and n states, P is the infrared power flux, and γ is the linewidth parameter (half width). For the same $\gamma = 10$ meV as used in Fig. 6 and assuming $f_{12} \sim 1$ and $f_{23} \sim 2$, the two-photon absorption efficiency for the double-resonance case is $\eta^{(2)}/P \sim 3 \times 10^{-10}$ $(\mathrm{W/cm^2})^{-1}$. The peak value in Fig. 6 for the solid curve is close to this value, and hence the case of bound-bound-continuum "resonant" configuration is close to the highest efficiency that we expect to achieve.

The only experimental study on two-photon absorption and photocurrent was reported in Refs. 26 and 7. The experimental proof of a two-photon detection is shown in Fig. 7. The QWIP signal is shown to be quadratically proportional to the Ge:Au (linear) monitor signal. The device was a standard 8-μm QWIP operated at 77 K. The situation is similar to the center part in Fig. 6. The pulse was from a CO_2 laser at 10.6 μm with a flat-top shape and 3-ps duration, generated by semiconductor optical switching.[7] Using the two-photon QWIP, an interferometric

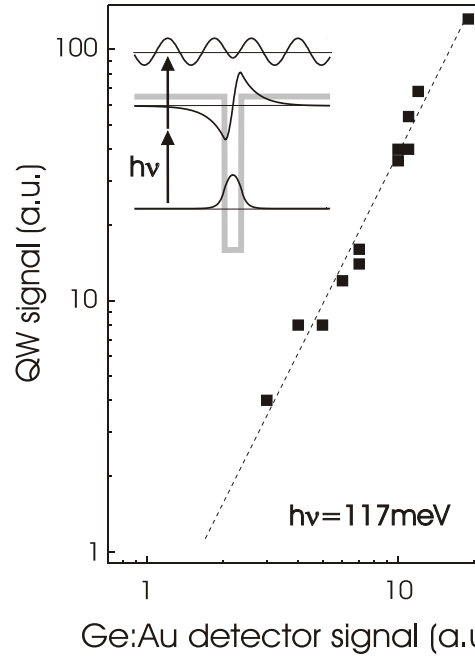

Fig. 7. QWIP signal versus reference detector signal under a pulse CO_2 laser with a wavelength of 10.6 μm. The inset shows the schematic quantum well potential and the two-photon absorption process.

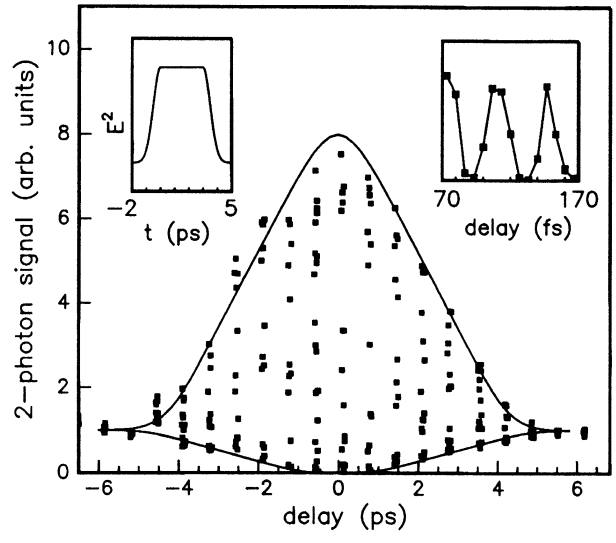

Fig. 8. Second-order interferometric autocorrelation trace of 3-ps-long pulses recorded every 0.67 ps during two or three oscillations each time. The solid curves are derived from the calculation of the envelope of the autocorrelation for destructive and constructive interferences, assuming a time-dependent intensity profile shown in the left inset. The right inset represents a zoom on a particular region of the autocorrelation trace.

autocorrelation trace of the pulse is shown in Fig. 8. The peak-to-background ratio of 8 : 1, characteristic of second-order autocorrelation, is clearly seen. Of particular interest is the use of a two-photon QWIP to characterize the pulses produced by mode-locked quantum cascade lasers.[8,27] This however may require a higher efficiency than the substantially detuned quantum well. Further work in this direction is underway.

4. Concluding Remarks

In general, the QWIP nonlinear properties and the intersubband nonlinear processes have not been extensively investigated. Here we provide an overview of nonlinear processes in QWIPs. This area as well as intersubband nonlinear optics should be further explored. In the short term, an optimized two-photon detector could be used to characterize pulses generated by quantum cascade lasers, and an improved difference frequency mixing scheme may generate sufficient terahertz powers of practical interest.

Acknowledgments

The authors thank H. Schneider for many fruitful discussions. One of us, H. C. Liu also thanks the Alexander von Humboldt Foundation for the Bessel Award.

References

1. H. C. Liu, "Quantum well infrared photodetector physics and novel devices," in *Intersubband Transition in Quantum Wells: Physics and Device Applications I*, eds. H. C. Liu and F. Capasso, Academic Press, San Diego, *Semiconductors and Semimetals*, Vol. 62, 2000, Chap. 3, pp. 126–196.
2. S. D. Gunapala and S. V. Bandara, "Quantum well infrared photodetector focal plane arrays," in *Intersubband Transition in Quantum Wells: Physics and Device Applications I*, eds. H. C. Liu and F. Capasso, Academic Press, San Diego, *Semiconductors and Semimetals*, Vol. 62, 2000, Chap. 4, pp. 197–282.
3. J. Y. Duboz, E. Costard, E. Rosencher, P. Bois, J. Nagle, J. M. Berset, D. Jaroszynski and J. M. Ortega, *J. Appl. Phys.* **77**, 6492 (1995).
4. J. Y. Duboz, E. Costard, J. Nagle, J. M. Berset, J. M. Ortega and J. M. Gérard, *J. Appl. Phys.* **78**, 1224 (1995).
5. M. Ershov, H. C. Liu, M. Buchanan, Z. R. Wasilewski and V. Ryzhii, *Appl. Phys. Lett.* **70**, 414 (1997).
6. H. C. Liu, J. Li, E. R. Brown, K. A. McIntosh, K. B. Nichols and M. J. Manfra, *Appl. Phys. Lett.* **67**, 1594 (1995).
7. A. Zavriyev, E. Dupont, P. B. Corkum, H. C. Liu and Z. Biglov, *Opt. Lett.* **20**, 1886 (1995).
8. R. Paiella, F. Capasso, C. Gmachl, D. L. Sivco, J. N. Baillargeon, A. L. Hutchinson, A. Y. Cho and H. C. Liu, *Science* **290**, 1739 (2000).
9. R. Martini, R. Paiella, C. Gmachl, F. Capasso, E. A. Whittaker, H. C. Liu, H. Y. Hwang, D. L. Sivco, J. N. Baillargeon and A. Y. Cho, *Electron. Lett.* **37**, 1290 (2001).
10. F. Capasso, R. Paiella, R. Martini, R. Colombelli, C. Gmachl, T. L. Myers, M. S. Taubman, R. M. Williams, C. G. Bethea, K. Unterrainer, H. Y. Hwang, D. L. Sivco,

A. Y. Cho, M. A. Sergent, H. C. Liu and E. A. Whittaker, *IEEE J. Quantum Electron.* **38**, 511 (2002).
11. H. C. Liu, J. Li, M. Buchanan and Z. R. Wasilewski, *IEEE J. Quantum Electron.* **32**, 1024 (1996).
12. H. C. Liu, R. Dudek, A. Shen, E. Dupont, C.-Y. Song, Z. R. Wasilewski and M. Buchanan, *Appl. Phys. Lett.* **79**, 4273 (2001).
13. T. Oogarah, H. C. Liu, E. Dupont, Z. R. Wasilewski, M. Byloos and M. Buchanan, *Semicond. Sci. Technol.* **17**, L41 (2002).
14. M. Ershov, V. Ryzhii and C. Hamaguchi, *Appl. Phys. Lett.* **67**, 3147 (1995).
15. M. Ershov, C. Hamaguchi and V. Ryzhii, *Jpn. J. Appl. Phys.* **35**, 1395 (1996).
16. H. C. Liu, L. Li, M. Buchanan and Z. R. Wasilewski, *J. Appl. Phys.* **82**, 889 (1997).
17. M. Ershov, H. C. Liu, A. G. U. Perera and S. G. Matsik, *Physica* **E7**, 115 (2000).
18. V. D. Shadrin, V. V. Mitin, V. A. Kochelap and K. K. Choi, *J. Appl. Phys.* **77**, 1771 (1995).
19. B. F. Levine, K. K. Choi, C. G. Bethea, J. Walker and R. J. Malik, *Appl. Phys. Lett.* **50**, 1092 (1987).
20. S. R. Schmidt, A. Seilmeier and H. C. Liu, *J. Appl. Phys.* **91**, 5545 (1999).
21. C. Mermelstein, H. Schneider, A. Sa'ar, C. Schönbein, M. Walther and G. Bihlmann, *Appl. Phys. Lett.* **71**, 2011 (1997).
22. J. E. Hubbs, D. C. Arrington, M. E. Gramer and G. A. Dole, *Opt. Eng.* **39**, 2660 (2000).
23. S. Schmidt, J. Kaiser and A. Seilmeier, *Physica* **B272**, 384 (1999).
24. H. C. Liu, J. Li, E. Costard, E. Rosencher and J. Nagle, *Solid State Electron.* **40**, 567 (199b).
25. C. Sirtori, F. Capasso, D. L. Sivco and A. Y. Cho, "Nonlinear optics in coupled-quantum-well quasi-molecules," in *Intersubband Transition in Quantum Wells: Physics and Device Applications II*, eds. H. C. Liu and F. Capasso, Academic Press, San Diego, *Semiconductors and Semimetals*, Vol. 67, 2000, Chap. 2, pp. 85–125.
26. E. Dupont, P. B. Corkum, H. C. Liu, P. H. Wilson, M. Buchanan and Z. R. Wasilewski, *Appl. Phys. Lett.* **65**, 1560 (1994).
27. R. Paiella, F. Capasso, C. Gmachl, H. Y. Hwang, D. L. Sivco, A. L. Hutchinson, A. Y. Cho and H. C. Liu, *Appl. Phys. Lett.* **77**, 169 (2000).